Rationally Designed N,N′-Bis[(N-p-guanidinobenzyl-N-methyl)aminocarbonyl]-1,3-diaminobenzene, "BIGBEN", Binds to the Minor Groove of d(CGCGAATTCGCG)$_2$ as Determined by Two-Dimensional Nuclear Magnetic Resonance Spectroscopy

Charles R. Watts,[†] Sean M. Kerwin,*[,‡] George L. Kenyon,[§] Irwin D. Kuntz,[§] and Deborah A. Kallick*[,†]

Contribution from the Department of Medicinal Chemistry, University of Minnesota, Minneapolis, Minnesota 55455, Division of Medicinal Chemistry, University of Texas at Austin, Austin, Texas, 78712, and Department of Pharmaceutical Chemistry, University of California at San Francisco, San Francisco, California, 94728

Received November 7, 1994[⊗]

Abstract: We have used homonuclear NMR techniques to investigate the interactions between the *de novo* designed minor groove ligand N,N′-bis[(N-p-guanidinobenzyl-N-methyl)aminocarbonyl]-1,3-diaminobenzene "BIGBEN" and the receptor for which it was designed, the d(CGCGAATTCGCG)$_2$ dodecamer. Our NMR results show unequivocally the interaction between the nonexchangeable and exchangeable protons of BIGBEN and the minor groove protons of the dodecamer. These interactions were characterized with the use of 1D NMR titrations to establish that the ligand is in fast-chemical exchange with the dodecamer on the chemical shift time scale, homonuclear NOESY experiments to establish the connectivities between the ligand and the DNA, and NOE-assisted computational modeling to develop a structural interpretation of the data. This represents the first complete iteration of our design cycle applied to the minor groove of DNA. The cycle begins with the selection of a receptor for which there is high-resolution structural data. A structural database is then searched for putative ligands which may have shape complementarity to the desired binding site on the receptor. The ligand, or a derivative thereof, is synthesized, and its ability to bind to the desired receptor is tested. The cycle culminates with the characterization of the structural interactions in the complex, elucidated here for BIGBEN and the dodecamer d(CGCGAATTCGCG)$_2$.

Introduction

There is a great deal of interest in designing novel ligands for biologically important receptors based primarily on knowledge of the three-dimensional structure of the receptor. This structure-based ligand design has the potential to greatly increase the number of lead compounds discovered for the development of new therapeutic agents. We have adopted a structure-based ligand design paradigm that is cyclical in nature.[1] In this paradigm, the structural information on the receptor is used to design putative ligands. These ligands, or their optimized derivatives, are synthesized and evaluated for binding to the target receptor. The evaluation process culminates in a structural interpretation of the binding mode of the ligand with the receptor. Through comparison of the predicted versus observed binding properties, rationally selected ligand modifications can then be employed in subsequent design cycles to improve both the design methodology and the binding affinity and selectivity of its resulting ligands. In practice, the application of this approach has been limited by the availability of the required three-dimensional structural information. Partly for this reason we have focused on a double stranded DNA dodecamer as a receptor. Solution NMR techniques can be used to obtain high resolution three-dimensional structural information of moderately sized oligonucleotides.and their respective ligands.[2,3] Thus, one need only know the sequence of interest, which can be synthesized via standard solid phase techniques in sufficient quantity for structural determination. The role of DNA as a *bona fide* receptor in targeted drug design has been discussed by Hurley.[4] A number of clinically important drugs exert their biological effects by binding to and/or covalently modifying DNA; however, the utility of these drugs is limited by their lack of selectivity.[5] An approach which views DNA as a target for structure based ligand design has the potential to result in the discovery of new classes of DNA ligands with increased selectivity and thus increased utility.

We have previously reported our initial efforts to apply the structure based ligand design paradigm to double stranded DNA targets.[6,7] We chose as a model system a well-studied double stranded DNA molecule of the sequence d(CGCGAATTCGCG)$_2$. Using the DOCK shape complementarity program, a subset of the Cambridge crystallographic database was

[†] University of Minnesota.
[‡] University of Texas at Austin.
[§] University of California at San Francisco.
[⊗] Abstract published in *Advance ACS Abstracts*, August 15, 1995.

(1) DesJarlais, R. L.; Sheridan, R. P.; Seibel, G. L.; Dixon, J. S.; Kuntz, I. D.; Venkataraghavan, R. *J. Med. Chem.* **1988**, 31, 722−729.

(2) Abbreviations: NMR, nuclear magnetic resonance spectroscopy; NOESY, two-dimensional nuclear Overhauser enhancement spectroscopy; NOE, nuclear overhauser effect; COSY, two-dimensional homonuclear shift-correlated spectroscopy; TSP 3-(trimethylsilyl)propionic-2,2,3,3-d_4 acid; BIGBEN, N,N′-bis[(N-p-guanidinobenzyl-N-methyl)aminocarbonyl]-1,3-diaminobenzene; AMBER, assisted model building and energy refinement.

(3) Searle, M. S. *Prog. in NMR Spect.* **1993**, 25, 403−480.

(4) Hurley, L. H. *J. Med. Chem.* **1989**, *32*, 2027−2033.

(5) Zimmer, C.; Wähnert, U. *Prog. Biophys. Mol. Biol.* **1986**, *47*, 31−112.

(6) Grootenhuis, P. D. J.; Kollman, P. A.; Seibel, G. L.; DesJarlais, R. L.; Kuntz, I. D. *Anti-Cancer Drug Design* **1990**, *5*, 237−242.

(7) Kerwin, S. M.; Kuntz, I. D.; Kenyon, G. L. *Med. Chem. Res.* **1991**, *1*, 361−369.

0002-7863/95/1517-9941$09.00/0

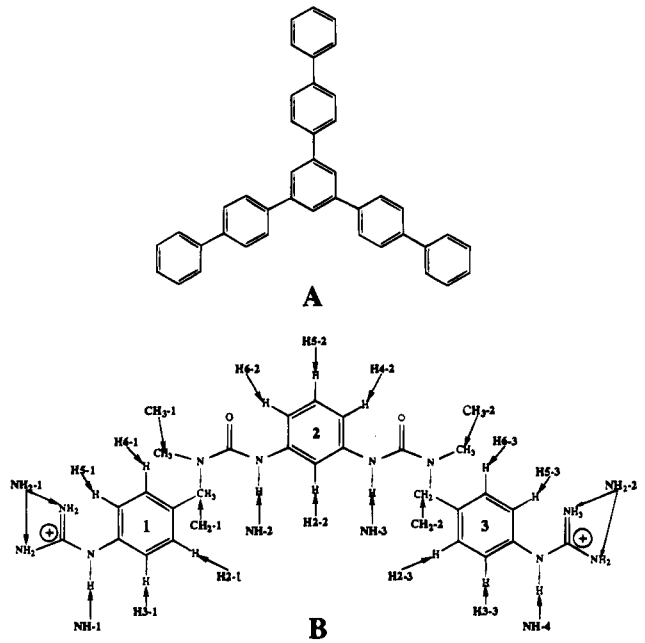

Figure 1. The result of the DOCK search of a subset of the Cambridge crystallographic database: (A) 1,3,5-tri(1,4-biphenyl)benzene and (B) the rationally designed minor groove binding agent *N,N'*-bis[(*N*-*p*-guanidinobenzyl-*N*-methyl)aminocarbonyl]-1,3-diaminobenzene, BIGBEN.

searched for known molecules that possess a shape which is complementary to the AT rich minor groove of the dodecamer. This search revealed a number of interesting molecules with a high degree of shape complementarity to the minor groove. One lead compound 1,3,5-tris(4-biphenylyl)benzene, Figure 1A, was used as a template to design the novel compound *N,N'*-bis[(*N*-*p*-guanidinobenzyl-*N*-methyl)aminocarbonyl]-1,3-diaminobenzene BIGBEN, shown in Figure 1B. The reengineering of the lead compound to produce BIGBEN was driven by attempts to retain, or even improve, the shape complementarity of the template, while introducing functionalities capable of hydrogen bonding and electrostatic interactions with the DNA receptor as well as water solubility.[7] BIGBEN is the first ligand of its kind in that it was designed to fit the DNA receptor from a computer shape complementarity search of a database. Evidence of minor groove binding has been previously offered by comparing the melting temperature of BIGBEN complexed to DNA with the melting temperatures of other minor groove binding agents as well as several competition binding assays.[7] In this paper we describe the characterization of the mode of binding of this rationally designed ligand using NMR spectroscopy and molecular mechanics and present two NMR derived models. This represents the first complete cycle of our structure-based design paradigm applied to DNA as a target receptor.

Material and Methods

Calculation of DNA Association Constants. Fluorescence measurements were obtained with a Hitachi model F-2000 spectrofluorimeter. The binding constants for BIGBEN were measured using the ethidium displacement technique under two different conditions. The concentration of ligand required to half the initial fluorescence of DNA-bound ethidium (C_{50}) was determined using the required DNA (0.5 μM base pairs) and ethidium (1.26 μM) in 20 mM sodium phosphate buffer. The degree of quenching of DNA-bound ethidium at a 1:1 ratio of ligand to ethidium (Q) was determined using an excess of the required DNA (20 μM base pairs) relative to ethidium (2 μM) in 20 mM phosphate buffer. The samples were excited at 546 nm, and the emission at 595 nm was measured for the ethidium alone, ethidium + DNA, and ethidium + DNA + varying amounts of ligand, added as a 2 mM solution in phosphate buffer. The association constants were calculated using a modification of the procedure reported by Cain and co-workers.[8] The fluorescence decrease in the C_{50} assay results from both displacement and quenching of DNA-bound ethidium by the ligand. When the added ligand concentration is sufficient to provide a 50% decrease in fluorescence

$$\frac{E_b}{E_{bo}}(100 - Q_x) = 50 \tag{1}$$

where Q_x is the percent decrease in ethidium fluorescence due to quenching, E_{bo} is the concentration of ethidium initially bound to DNA before any added ligand, and E_b is the concentration of ethidium bound to DNA after addition of sufficient ligand to halve the initial fluorescence. E_{bo} is calculated given the total amount of ethidium in the assay and the association constant for ethidium by applying eq 2

$$E_b = K_E(E_t - E_b)S_{fE} \tag{2}$$

where K_E is the association constant for ethidium (9.5×10^6 M^{-1} for poly(dAdT)$_2$, 9.9×10^6 M^{-1} for poly(dCdG)$_2$), E_t is the total concentration of ethidium, and S_{fE} is the concentration of free ethidium intercalation sites on the DNA. S_{fE} is given by the site-exclusion treatment of McGhee and von Hippel

$$S_{fE} = S_t \times \frac{\left\{1 - \left[n_E\left(\frac{E_b}{S_t}\right) + n_D\left(\frac{D_b}{S_b}\right)\right]\right\}^{n^E}}{\left\{1 - \left[(n_E - 1)\frac{E_b}{S_t} + (n_D - 1)\left(\frac{D_b}{S_t}\right)\right]\right\}^{(n_E-1)}} \tag{3}$$

where S_t is the total concentration of DNA in base pairs, D_b is the concentration of ligand bound to DNA, n_E is the DNA binding site size for ethidium in base pairs, and n_D is the binding site size for the added ligand ($n_E = 2$, $n_D = 4$ for BIGBEN or 5 for distamycin).[9] Using eq 1, E_b can be calculated for any Q_x. Using this E_b, D_b can be calculated using eqs 2 and 3 and the relationship $n_E E_b + n_D D_b < S_t$.

Q_x is first estimated from Q by assuming that all of the ligand added in determining Q is bound to DNA. The amount of ethidium bound in the quenching assay (E_{bq}) is then calculated by applying eqs 2 and 3. Q_x is then estimated using eq 4.

$$Q_x = Q - 100\left(\frac{E_{bq}}{E_{bqo}}\right) \tag{4}$$

Using eqs 1, 2, and 3, E_b and D_b for the displacement assay is obtained for the Q_x calculated using eq 4. The association constant of the ligand (K) is then calculated using eq 5.

$$K = \frac{K_E D_b(E_t - E_b)}{E_b(D_t - D_b)} \tag{5}$$

This K is used to estimate D_{bq}, the actual amount of ligand bound in the determination of Q, using eq 6

$$\left(\frac{D_{bq}}{D_{tq}}\right) = \frac{S_{fDK}}{(1 + S_{fD}K)} \tag{6}$$

where S_{fD}, the concentration of free ligand binding sites, is given by the counterpart of eq 3. This new value of D_{bq} for the quenching assay is used to calculate a corresponding value of E_{bq} using eqs 2 and 3. Using this new value of E_{bq}, a new estimate of Q_x is obtained by applying eq 4. A new value for K is then calculated, and the whole process is repeated until convergence is reached. All association constant values reported represent the average of three separate determinations.

(8) Baguley, B. C.; Denny, W. A.; Atwell, G. J.; Cain, B. F. *J. Med. Chem.* **1981**, *24*, 170–177.
(9) McGhee, J. D.; von Hippel, P. H. *J. Mol. Biol.* **1974**, *86*, 469–489.

NMR Sample Preparation. The DNA oligonucleotide d(CGCGAATTCGCG)$_2$ was either purchased from Midland Inc. or synthesized and purified in the lab of L. H. Hurley (U.T. Austin). NMR samples were prepared by dialyzing the oligonucleotide against HPLC grade water, lyophilizing to dryness, and redissolving in 500 μL of buffer solution containing: 10 mM phosphate, 100 mM NaCl, 0.01% NaN_3, and 0.02% TSP (used as the chemical shift standard). After adjusting the pH to 7.0, the samples were passed through a sterile 0.22 μM syringe filter after which the exchangeable protons were replaced with deuterons by lyophilizing twice with 99.9% D_2O (Cambridge Isotope Laboratories). The concentration of oligonucleotide was determined using the calculated extinction coefficient $\epsilon_{260} = 114\,020\ M^{-1}\ cm^{-1}$.[10] The final DNA sample was 1.65 mM d(CGCGAATTCGCG)$_2$, 10 mM phosphate, 100 mM NaCl, 0.01% NaN_3, 0.02% TSP, pH 7.00 in 90% D_2O, 10% 1,4-dioxane-d_8. We found that dioxane facilitated the solubility of the ligand and did not appreciably change the chemical shifts of the oligonucleotide.

The ligand *N,N'*-bis[(*N*-*p*-guanidinobenzyl-*N*-methyl)aminocarbonyl]-1,3-diaminobenzene BIGBEN was synthesized as the hydrochloride salt as described previously.[7] BIGBEN was dissolved in 500 μL of 10 mM phosphate, 100 mM NaCl, 0.01% NaN_3, 0.02% TSP, and 10% 1,4-dioxane-d_8 buffer. The pH of the solution was adjusted to 7.0 before being passed through a sterile 0.22 μM syringe filter. The exchangeable protons were replaced with deuterons by lyophilizing twice with 99.9% D_2O (Cambridge Isotope Laboratories). The concentration of BIGBEN was determined using the extinction coefficient $\epsilon_{234} = 34\,830\ M^{-1}\ cm^{-1}$.[7] The final ligand sample was 15.65 mM BIGBEN, 10 mM phosphate, 100 mM NaCl, 0.01% NaN_3, 0.02% TSP, pH 7.00 in 90% D_2O, 10% 1,4-dioxane-d_8.

One-Dimensional NMR Titration. Titration of the ligand into the DNA was performed on a Bruker AMX-500 spectrometer equipped with an Aspect X32 workstation and analyzed using the FELIX module of Biosym software on a Silicon Graphics Personal Iris. BIGBEN was added to the NMR sample containing the DNA in 0.25 mol equiv steps and monitored by acquiring one-dimensional spectra of the nonexchangeable protons for each titration point. The nonexchangeable protons were observed at 10 °C using 8K complex points, 1024 scans, a spectral width of 6024.096 Hz, and a relaxation delay of 2,5 s.

Two-Dimensional NMR. Two-dimensional NOESYs of the nonexchangeable protons were collected on either a Bruker AMX-500 or Varian UNITY 600 MHz spectrometer. The NOESYs for an NOE build-up curve were obtained sequentially at 500 MHz and 10 °C, with mixing times of 50, 100, and 150 ms. The standard NOESY pulse sequence with 2K complex points, 512 t_1 increments, 64 scans per t_1, a spectral width of 6024.096 Hz, a relaxation delay of 2 s, and hyper complex phase cycling was used.[11,12] Final assignment of the nonexchangeable cross peaks were verified with a NOESY collected at 600 MHz, at 10 °C, using 2 K complex points, 1024 t_1 increments, 32 scans per t_1, spectral width of 8000 Hz, mixing time of 200 ms, relaxation delay of 2 s, and hyper complex phase cycling. The exchangeable protons were observed in the following manner. The titrated ligand·DNA sample was lyophilized to dryness then re dissolved in 80% H_2O, 10% D_2O, 10% 1,4-dioxane-d_8 and adjusted to pH 5.8. The final sample concentration was 1.49 mM BIGBEN·d(CGCGAATTCGCG)$_2$, 10 mM phosphate, 100 mM NaCl, 0.01% NaN_3, and 0.02% TSP. Spectra were obtained at 600 MHz on a Bruker AMX-600 spectrometer equipped with a gradient blanking unit using a 3-9-19 pulse and tailored gradients to achieve suppression of the H_2O peak.[13,14] Spectra were obtained at 5° C with mixing times of 100 and 200 ms using 2K complex points, 1024 t_1 increments, 32 scans per t_1, a spectral width of 12 820.513 Hz, a relaxation delay of 2 s, and TPPI phase cycling.[15]

All two-dimensional data were analyzed using the FELIX module of Biosym software on a Silicon Graphics Personal Iris. Typical data were apodized in both dimensions with a skewed sine bell squared function (1024 points, 90° phase shift, 0,9 skew in t_2 and 256−512 points, phase 90°, skew 0.9 in t_1). The first FID was multiplied by 0.5 before Fourier transformation of the t_1 dimension.

Computational Modeling. Two models of interaction were built for the BIGBEN·d(CGCGAATTCGCG)$_2$ complex using constrained molecular dynamics and mechanics calculations taking into consideration the originally selected binding site, the NMR titration data, the NOESY derived NOE constraints, and the subsequent computational modeling of the preferred binding site and ligand conformation using a interactive combination of Sybyl, DOCK, and AMBER. All molecular dynamics and mechanics calculations were performed using the SANDER module of AMBER v4.0 with standard partial charges being applied to the DNA unless otherwise noted.[16,17] Partial atomic charges for BIGBEN were derived from MOPAC ESP calculations or taken from those published for urea,[18,19] Bond length, bond angle, and dihedral angle parameters were derived from equilibrium values determined from X-ray crystal structures of urea and symdiphenyl urea or adapted from values published by Alagon and co-workers.[20−22] The complete AMBER parameters for BIGBEN are included in the supporting information. The charge neutrality of the system was maintained by placing sodium counterions 3.0 Å from the bisectors of the phosphates and chloride ions using Jorgenson's parameters 3.0 Å from the bisectors of BIGBEN's terminal guanidino groups.[23] Correct hydrogen bond distance and geometry between base pairs was enforced by applying a 5.0 (kcal/mol)/Å^2 harmonic potential with equilibrium distance of 2.9 Å between donor and acceptor atoms and equilibrium bond angle of 180° between the donor, donated hydrogen, and acceptor atoms. All calculations were performed using a distance dependent dielectric of the form $\epsilon = r$ to simulate the effect of solvent shielding and an infinite cutoff distance for generation of the nonbonded atom list. The resulting data was analyzed using InsightII and the static energies of interaction between the ligand and the oligonucleotide were deconvoluted with the ANAL module of AMBER v4.0.

(a) Generation of Symmetric Model. The ligand was interactively docked to the minor groove of canonical B-form DNA guided by the 40 observed intermolecular NOEs using the three-dimensional graphical interface of Insight II v2.3.[24−26] The docked structure was then refined with respect to the fixed field of the DNA using a modified version of the combined molecular mechanics and dynamics protocol described by Brünger and used in other ligand·DNA NMR studies.[27−29] The protocol consisted of 200 steps of steepest descent minimization, 0.1 ps of dynamics raising the temperature from 0 to 300 K, 1 ps of constant temperature dynamics at 300 K, and 200 steps of steepest descent minimization followed by 2000 steps of conjugate gradient minimization. This process was repeated 10 times, gradually increasing the strength of the flat-well harmonic potentials enforcing the observed NOE constraints from 1 to 200 (kcal/mol)/Å^2. The constraints were

(10) Warshaw, M. M.; Cantor, C. R. *Biopolymers* **1970**, *9*, 1079−1103.
(11) Macura, S.; Ernst, R. R. *Mol. Phys.* **1980**, *41*, 95−117.
(12) States, D. J.; Haberkorn, R. A.; Ruben, D. J. *J. Magn. Reson.* **1982**, *48*, 286−292.
(13) Sklenar, V.; Piotto, M.; Leppik, R.; Saudek, V. *J. Magn. Reson., Series A* **1993**, *102*, 241−245.
(14) Piotto, M.; Saudek, V.; Sklenar, V. *J. Biomol. NMR* **1992**, *2*, 661−665.
(15) Marion, D.; Wüthrich, K. *Biochem. Biophys. Res. Comm.* **1983**, *113*, 967−974.
(16) Pearlman, D. A.; Case, D. A.; Caldwell, J. C.; Seibell, G. L.; Singh, U. C.; Weiner, P.; Kollman, P. A. AMBER 4.0; University of California, San Fransisco, 1991.
(17) Weiner, S. J.; Kollman, P. A.; Nguyen, D. T.; Case, D. A. *J. Comput. Chem.* **1986**, *7*, 230−252.
(18) Stewart, J. J. P. *J. Comp.-Aided Mol. Des.* **1990**, *4*, 1−105.
(19) Kuharski, R. A.; Rossky, P. J. *J. Am. Chem. Soc.* **1984**, *106*, 5786−5793.
(20) Andrew, E. R.; Hyndman, D. *Disc. Faraday Soc.* **1955**, *19*, 195−200.
(21) Dannecker, W.; Kopf, J.; Rust, H. *Cryst. Struct. Comm.* **1979**, *8*, 429−432.
(22) Algona, G.; Ghio, C. *J. Comput. Chem.* **1991**, *12*, 934−942.
(23) Jorgensen, W. L.; Buckner, J. K.; Huston, S. E.; Rossky, P. J. *J. Am. Chem. Soc.* **1987**, *109*, 1891−1899.
(24) Blaskó, A.; Browne, K. A.; He, G.-X.; Bruice, T. C. *J. Am. Chem. Soc.* **1993**, *115*, 7080−7092.
(25) Arnott, S.; Chandrasekaram, R.; Hall, I.; Puigjaner, L. C. *Nucleic Acids Res.* **1983**, *11*, 4141−4155.
(26) Insight II User Guide, version 2.3.0, San Diego: Biosym Technologies, 1993.
(27) Brünger, A. T. In *Molecular Dynamics: Applications in Molecular Biology* Goodfellow, J. M., Ed.; Macmillan Press, London, 1990; pp 137−178.
(28) Parkinson, J. A.; Ebrahimi, S. E.; McKie, J. H.; Douglas, K. T. *Biochemistry* **1994**, *33*, 8442−8452.
(29) Lane, A. N.; Jenkins, T. C.; Brown, T.; Neidle, S. *Biochemistry* **1991**, *30*, 1372−1385.

then removed, and the entire system was energy minimized with 1000 steps of steepest descent minimization followed by conjugate gradient minimization until the change in energy per iteration was less than 0.0001 kcal/mol.

(b) Generation of Offset Model. The Sybyl molecular modeling package was used to generate 56 000 low energy conformations of BIGBEN by systematic rotation about all rotatable bonds in 15° to 30° increments.[30,31] These conformations were grouped into 16 families based upon intrafamily similarity in the torsion angles between the two central C(Ar)−N(H) bonds. One thousand of the lowest energy conformations from each of the families were searched by DOCK v3,0 using the X-ray structure of the dodecamer as the receptor, with partial atomic charges for the DNA as calculated from X-ray diffraction data.[32−34] The single conformation from each family that received the most favorable DOCK score was subjected to AMBER minimization within the fixed field of the DNA receptor, and the resulting minimized conformations were reDOCKed into the DNA.

The combined use of Sybyl, DOCK, and AMBER described above indicated that BIGBEN should bind more favorably if offset one base pair in either the 5′ or 3′ direction from the central 5′AATT3′ binding site. The model of offset binding was refined with respect to the fixed field of the DNA from the interactively docked starting structure of part (a) using repetitive cycles of a simulated annealing protocol that consisted of cooling the system from 1000 to 0 K over a period of 20 ps, while gradually increasing the strength of the flat-well harmonic NOE constraints from 1 to 200 (kcal/mol)/Å^2.[35] This process was repeated several times to determine which NOEs could be obeyed in the offset complex. The constraints were then removed, and the entire system energy was minimized with 1000 steps of steepest descent minimization followed by conjugate gradient minimization until the change in energy per iteration was less than 0.0001 kcal/mol.

Results

Equilibrium Constant. We employed the ethidium displacement method to calculate an apparent association constant for BIGBEN binding to poly(dAdT)$_2$ ($K = 2.0 \pm 0.2 \times 10^5$ M^{-1}) and poly(dCdG)$_2$ ($K = 6.5 \pm 0.3 \times 10^4$ M^{-1}) showing a slight preference for AT rich DNA. These may be compared to distamycin, for which we calculate an apparent association constant for poly(dAdT)$_2$ of $3.9 \pm 0.2 \times 10^8$ M^{-1}. Our calculated apparent association constant for distamycin and poly(dAdT)$_2$ is somewhat lower than reported association constants determined from UV melting curves, $K = 2.6 \pm 0.9 \times 10^9$ M^{-1}.[35,36] This underestimation of the association constants for very tight binding ligands is a well-recognized limitation of the ethidium displacement assay.[37] Although BIGBEN binds to AT-rich DNA much less tightly than distamycin, based on the concentrations we have used in our NMR experiments, the fraction dissociated in the NMR tube is estimated to be less than 10%.

One-Dimensional NMR Titration. Addition of BIGBEN to the oligonucleotide causes gradual changes in the chemical shift and a broadening of the proton resonances of the DNA and the ligand. These changes are evident by examining the downfield region of the proton NMR titration spectra which includes the cytosine C6H, adenine C2H and C8H, guanine C8H, and thymine C6H resonances as well as those of the aromatic protons on rings one, two, and three of the ligand as shown in Figure 2. The first 0.25 mol equiv addition of BIGBEN to the oligonucleotide causes several notable changes in the spectrum: the appearance of two small, broad peaks at 7,10 and 7,45 ppm due to the ligand and a downfield shift of the DNA's A5C2H/A17C2H and A6C2H/A18C2H minor groove protons.[38] Further addition of BIGBEN causes the ligand resonances to grow in intensity and both the DNA and ligand resonances to gradually change in chemical shift. The chemical shift changes for the central six base pairs are reported in Table 1. We have not reported the negligible changes for the first three residues (less than 0.05 ppm). The change in chemical shifts caused by formation of the complex are relatively small with the greatest change evident for the minor groove protons of residues A6/A18 through C9/C21. The greatest chemical shift change is −0.22 ppm and is observed for the minor groove T7C4′H proton.

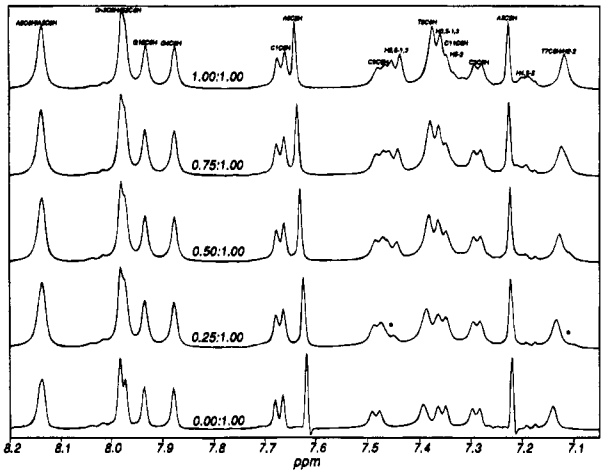

Figure 2. Expansion of the downfield region of the one-dimensional ^{1}H NMR spectra illustrating the quantitative titration of BIGBEN into d(CGCGAATTCGCG)$_2$ at 500 MHz. Resonances corresponding to the ligands H2-2 and H2,6-1,3 protons are marked at the 0.25:1.00 BIGBEN:DNA ratio with asterisks (*).

The titration behavior indicates that the ligand is in fast exchange on the chemical shift time scale with its binding site on the oligonucleotide. This fast exchange behavior cannot be changed to a slow or intermediate regime by altering the temperature of the system (data not shown). The absence of an increase (except those accounted for by addition of the ligand) or doubling of the number of observed resonances during the titration indicates that the overall symmetry of the ligand and DNA is maintained in the complex on the NMR time scale.

Two-Dimensional NMR. The uncomplexed oligonucleotide resonances were assigned using the sequential assignment technique and verified to be consistent with the previous assignments.[38] This process was then repeated for the ligand:DNA complex at the 1.00:1.00 mol equivalency ratio, the assignments of which are summarized in Table 2. All cross peaks in the complex were negative, confirming that BIGBEN is bound to the DNA and is on average governed by the oligonucleotide's macromolecular motions. The negligible perturbations in chemical shift of protons outside of the minor groove as well as the observation of all NOE connectivities characteristic of B-DNA indicate that the binding of BIGBEN minimally perturbs the overall structure of the oligonucleotide.

Assignment of the oligonucleotide's resonances allowed for those of the ligand to be assigned partly by a process of

(30) Clark, M.; Cramer III, R. D.; Van Opdenbosch, N. *J. Comput. Chem.* **1989**, *10*, 982−1012.
(31) SYBYL, version 5.5; Tripos Associates, Inc.: St. Louis, MO, 1992.
(32) Meng, E. C.; Shoichet, B. K.; Kuntz, I. D. *J. Comput. Chem.* **1992**, *13*, 505−524.
(33) Kopka, M. L.; Yoon, C.; Goodsell, D.; Pjura, P.; Dickerson, R. E. *Proc. Natl. Acad. Sci. U.S.A.* **1985**, *82*, 1376−1380.
(34) Pearlman, D. A.; Kim, S. *J. Mol. Biol.* **1990**, *221*, 171−187.
(35) Breslauer, K. J.; Remeta, D. P.; Chou, W.-Y.; Ferrante, R.; Curry, J.; Zaunczkowski, D.; Snyder, J. G.; Marky, L. A. *Proc. Natl. Acad. Sci. U.S.A.* **1987**, *84*, 8922−8925.
(36) Rentzeperis, D.; Kupke, D. W.; Marky, L. A. *Biopolymers* **1992**, *32*, 1065−1075.
(37) Morgan, A. R.; Lee, J. S.; Pulleyblank, D. E.; Murry, N. L.; Evans, D. H. *Nucleic Acids Res.* **1979**, *7*, 547−569.

(38) Our numbering of the oligonucleotide d(CGCGAATTCGCG)$_2$ is the same as that of Hare, D. R.; Wemmer, D. E.; Chou, S.; Drobny, G.; Reid, B. R. *J. Mol. Biol.* **1983**, *171*, 319−336.

Table 1. Change in Chemical Shift (ppm) of Selected Nonexchangeable Proton Resonances of the Oligonucleotide d(CGCGAATTCGCG)$_2$ and Ligand *N,N'*-Bis[(*N*-*p*-guanidinobenzyl-*N*-methyl)aminocarbonyl]1,3-diaminobenzene BIGBEN at a 1.00:1.00 Mol Equivalency Ratio[a]

DNA proton	Δppm	ligand proton	Δppm
G4C8H/G16C8H	0.01	H2-1	+0.05
G4C1′H/G16C1″H	−0.06	H3-1	+0.03
G4C2′H/G16C2′H	−0.02	H5-1	+0.03
G4C2″H/G16C2″H	−0.03	H6-1	+0.05
G4C4′H/G16C4′H	−0.03	CH2-1	+0.05/−0.03
A5C2H/A17C2H	+0.01	CH3-1	−0.04
A5C8H/A17C8H	−0.01	H2-2	−0.18
A5C1′H/A17C1′H	−0.04	H4-2	+0.12
A5C2′H/A17C2′H	−0.02	H5-2	+0.01
A5C2″H/A17C2″H	−0.03	H6-2	+0.12
A5C4′H/A17C4′H	−0.04	CH2-2	+0.05/−0.03
A6C2H/A18C2H	+0.03	CH3-2	−0.04
A6C8H/A18C8H	−0.01	H2-3	+0.05
A6C1′H/A18C1′H	−0.04	H3-3	+0.03
A6C2′H/A18C2′H	−0.02	H5-3	+0.03
A6C2″H/A18C2″H	−0.07	H6-3	+0.05
A6C4′H/A18C4′H	−0.09		
T7C6H/T19C6H	−0.03		
T7CH3/T19CH3	−0.02		
T7C1′H/T19C1′H	−0.11		
T7C2′H/T19C2′H	−0.05		
T7C2″H/T19C2″H	−0.10		
T7C4′H/T19C4′H	−0.22		
T8C6H/T20C6H	−0.03		
T8CH3/T20CH3	−0.03		
T8C1′H/T20C1′H	−0.09		
T8C2′H/T20C2″H	−0.05		
T8C2″H/T20C2″H	−0.08		
T8C4′H/T20C4′H	−0.16		
C9C5H/C21C5H	−0.03		
C9C6H/C21C6H	−0.02		
C9C1′H/C21C1′H	−0.07		
C9C2′H/C21C2′H	−0.04		
C9C2″H/C21C2″H	−0.04		
C9C4′H/C21C4′H	−0.09		

[a] Numbering of the oligonucleotide d(CGCGAATTCGCG)$_2$ is the same as that of Hare, D. R.; Wemmer, D. E.; Chou, S.; Drobny, G.; Reid, B. R. *J. Mol. Biol.* **1983**, *171*, 319-336.

elimination. This was also facilitated by the data available from the NOE build-up experiments which allowed for a semiquantitative interpretation of the cross-peaks. The following is a description of the ligand assignments in the complex and is summarized in Table 3, with the ligand nomenclature described in Figure 1. The H2-2 proton was assigned on the basis of a medium NOE to the H4-2 and H6-2 protons and weak NOEs to the H5-2 and CH_3-1,2 protons. The CH_3-1,2 protons were assigned on the basis of a medium NOE to the CH_2-1,2 protons and weak NOEs to the H2-2, H2-1,3, and H6-1,3 protons. The CH_2-1,2 protons were assigned on the basis of medium NOEs to the CH_3-1,2, H2-1,3, and H6-1,3 protons and a weak NOE to the H3-1,3 and H5-1,3 protons. The CH_2-1,2 resonance also changed from a degenerate resonance in the free ligand to two nondegenerate resonances in the presence of the oligonucleotide. The aromatic protons on rings one and three were assigned on the basis of two degenerate resonances representing the H2-1,3 and H6-1,3, and H3-1,3 and H5-1,3 protons with a medium NOE between the H2-1,3 and H6-1,3, and CH_2-1,2 protons and a weak NOE between the H3-1,3 and H5-1,3, and CH_2-1,2 protons. The degeneracy of the aromatic protons on rings one and three and the nondegenerate CH_2-1,2 resonances indicates that the rings rotate rapidly (>200 Hz) around the bond between the methylene and phenyl moieties,[39]

Similarly, the exchangeable protons of the ligand could be assigned using the two-dimensional data available from the NOESYs collected in H_2O (data not shown). The NH-2,3 protons were assigned via medium NOEs to the H2-2 and CH_3-1,3 protons. The NH-1,4 protons were assigned on the basis of medium NOEs to the H3-1,3, and H5-1,3, and NH_2-1,2 protons. The NH_2-1,2 protons were assigned on the basis of a medium NOE to the NH-1,4 protons and a weak NOE to the H3-1,3 and H5-1,3 protons. The exchangeable protons on the ligand were not observed in the absence of DNA. The complete proton assignments for BIGBEN in the complex are given in Table 3.

Assignment of the proton resonances of the oligonucleotide and BIGBEN allowed for assignment of the intermolecular crosspeaks. Representative NOESY spectra are shown in Figures 3 and 4. Twenty intermolecular NOEs are observed; all between the ligand and the minor groove. The observed NOEs are summarized in Table 3 and show unequivocally that BIGBEN binds in the minor groove of the dodecamer. Some of the key ligand-to-DNA NOEs that indicate minor groove binding are as follows; H2-2→A6C2H, A18C2H, T8C1′H, and T20C1′H; CH_3-1→A5C2H, A6C2H, T19C1′H, and T20C1′H; CH_3-2→A17C2H, A18C2H, T7C1′H, and T8C1′H; H2,6-1→A6C2H, H2,6-3→A18C2H, H3,5-1→A5C2H and A6C2H, and H3,5-3→A17C2H and A18C2H. We note that the methyl groups on the ligand point into the minor groove, as shown by the NOEs in Figure 4. It was impossible to determine if an NOE cross peak was present between the H2−2 and T7C1′H/T19C1′H protons due to spectral overlap, but the T7C1′H/T19C1′H protons experience a 0.11 ppm shift upon ligand complexation. The NOEs between rings one and three and the minor groove adenine C2H protons are observable only at 600 MHz and are not apparent at 500 MHz. The minor groove

Table 2. Resonance Assignments of the Exchangeable and Nonexchangeable Protons of BIGBEN;d(CGCGAATTCGCG)$_2$ = 1.0:1.0[a-c]

residue	N3H	C4NH$_2$	C5H	C6H	CH$_3$	N1H	C2NH$_2$	C6NH$_2$	C2H	C8H	C1′H	C2′H	C2″H	C3′H	C4′H
C1		8.30	5.91	7.66							5.73	1.97	2.42	4.71	4.05
G2						13.12	6.69			7.96	5.89	2.65	2.71	4.97	4.34
C3		8.42	5.37	7.28							5.58	1.85	2.27	4.81	4.12
G4						12,73	6.90			7.87	5.42	2.67	2.76	4.99	4.31
A5								*d*	7.22	8.13	5.99	2.71	2.93	5.06	4.44
A6								*d*	7.64	8.14	6.16	2.56	2.91	4.99	4.42
T7	13.71			7.12	1.26						5.88	1.98	2.53	4.79	4.10
T8	13.82			7.38	1.52						6.07	2.15	2.52	4.87	4.11
C9		8.45	5.61	7.47							5.61	1.97	2.40	4.87	4.11
G10						12.94	6.54			7.93	5.85	2.65	2.70	4.98	4.33
C11		8.52	5.44	7.35							5.73	1.91	2.32	4.82	4.15
G12						13.26	7.15			7.98	6.16	2.64	2.34	4.68	4.18

[a] Nonexchangeable protons were assigned in 10 mM PO_4^{3-}, 100 mM NaCl, 0.01% NaN_3, 90% D_2O, and 10% 1,4-dioxne-d_8, pD 7.00 at 10 °C. [b] Exchangeable protons were assigned in 10 mM PO_4^{3-}, 100 mM NaCl, 0.01% NaN_3, 80% H_2O, 10% D_2O, and 10% 1,4-dioxane-d_8, pH 5.50 at 10 °C. [c] The C5′H and C5″H ribose protons of the oligonucleotide were not assigned due to spectral overlap. [d] The A5C6NH$_2$ and A6C6NH$_2$ proton resonances were not assignable.

Table 3. Observed Proton Chemical Shifts for BIGBEN and Intermolecular NOEs for BIGBEN·d(CGCGAATTCGCG)$_2$

proton	ppm	NOE	NOE	NOE	NOE	NOE	NOE
NH_2-1	9.34						
NH-1	7.07	C21C4′H					
H2-1	7.45	A6C2H	C21C4′H				
H3-1	7.38	A5C2H	A6C2H				
H5-1	7.38	A5C2H	A6C2H				
H6-1	7.45	A6C2H	C21C4′H				
CH_2-1	4.60/4.67						
CH_3-1	3.04	A5C2H	A6C2H	T7C1′H	T20C1′H	C21C1′H	C21C4′H
NH-2	8.22	A6C2H	T20C4′H				
H2-2	7.06	A6C2H	A18C2H	A6C4′H	A18C4′H	T8C1′H	T20C1′H
H4-2	7.21						
H5-2	7.32						
H6-2	7.21						
NH-3	8.22	A18C2H	T8C4′H				
CH_2-2	4.50/4.67						
CH_3-2	3.04	A17C2H	A18C2H	T8C1′H	T19C1′H	C9C1′H	C9C4′H
H2-3	7.45	A18C2H	C9C4′H				
H3-3	7.38	A17C2H	A18C2H				
H5-3	7.38	A17C2H	A18C2H				
H6-3	7.45	A18C2H	C9C4′H				
NH-4	7.07	C9C4′H					
NH_2-2	9.34						

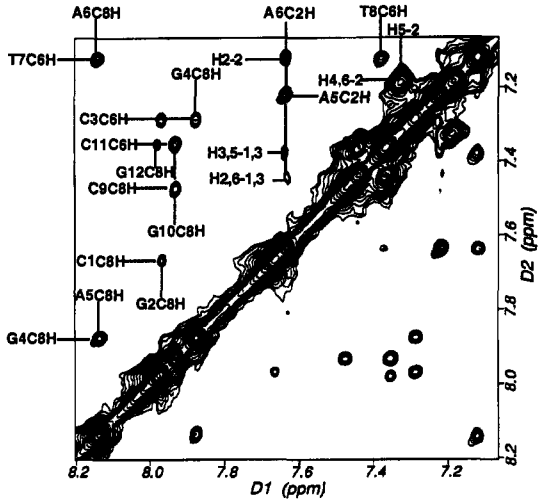

Figure 3. Expansion of the aromatic region of the NOESY at 600 MHz, 10 °C, 200 ms mixing time, 1.0:1.0 BIGBEN:DNA, in 90% D_2O and 10% 1,4-dioxane-d_8. The NOEs from the protons on rings one and three of BIGBEN to the A6C2H and the H2-2 proton to A6C2H are clearly visible in this region. The NOEs from rings one and three were not observed at any mixing time at 500 MHz.

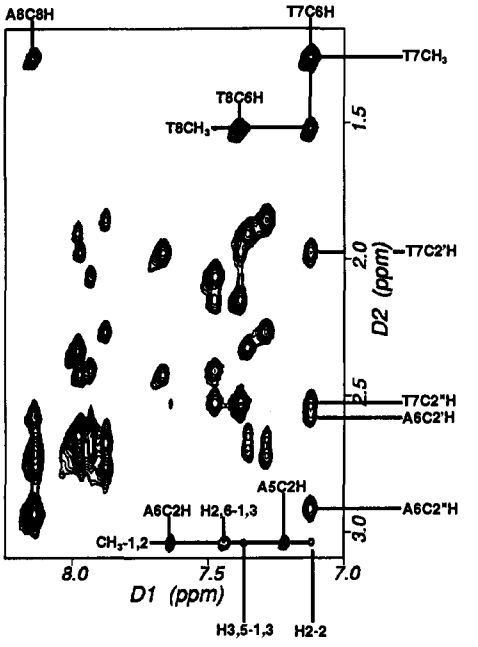

Figure 4. Expansion of the aromatic to C2′H, C2″H region of the NOESY at 500 MHz, 10 °C, 200 ms mixing time, 1.0:1.0 BIGBEN: DNA, in 90% D_2O and 10% 1,4-dioxane-d_8. The NOEs from the CH_3-1,2 protons to A5C2H, A17C2H, A6C2H, and A18C2H show the interaction of the *N*-methyl moiety with the floor of the minor groove. All the unlabeled cross peaks are due to the regular B-DNA connectivities expected and previously assigned in this spectral region.

binding mode is further verified by the NOEs between the ligand's exchangeable protons and the minor groove. The NOEs between the NH-2→A5C2H and NH-3→A17C2H protons may indicate that this ligand amide moiety is in the proximity of the thymine O2 and adenine N3 hydrogen bond acceptor atoms, deep within the minor groove. We also observe NOEs between the ligand terminal NH-1, NH-4 and the DNA C21C4′H, C9C4′H, respectively. None of the NH protons on the ligand were observable in the free ligand.

The NOE build-up curve also contains important information for the characterization of the binding mode of BIGBEN to the oligonucleotide, shown in Figure 5. Comparison of the intermolecular NOEs to selected intramolecular NOEs of the DNA shows that the intermolecular NOEs are much weaker and build up over a longer time period. This weak NOE intensity may be caused by the averaging of both the R_1 and σ relaxation rates, which occurs when exchange is fast on both the chemical shift and T_1 relaxation time scales.[40] We do not observe any exchange NOEs, suggesting that the residence time at each site must be long enough to be observed via cross peaks in the NOESY but too fast to be observed via exchange NOEs.

Although the NMR data unequivocally demonstrate minor groove binding, it is instructive to note that the ligand does not bind in the conformation that was assumed in the design process. A best-fit superposition of the central aromatic ring and terminal benzyl groups of BIGBEN onto the central and two terminal phenyl rings in the lead compound (Figure 1) produces a conformation with both urea *N*-methyl groups oriented *cis* to the carbonyl oxygens (N-Me "out" conformation, Figure 6B).

(39) Searle, M. S.; Embrey, K. J. *Nucleic Acids Res.* **1990**, *18*, 3753–3762.

(40) Neuhaus, D.; Williamson, M. *The Nuclear Overhauser Effect in Structural and Conformational Analysis*; VCH: New York, 1989.

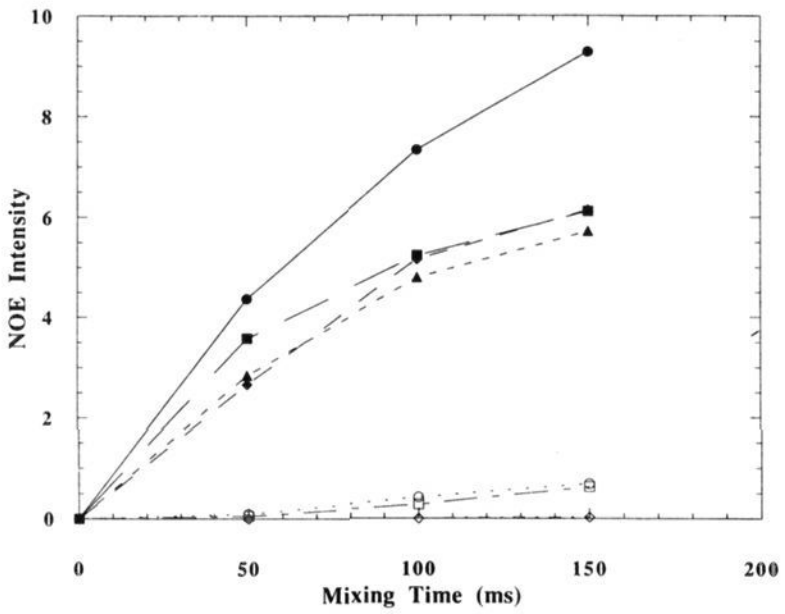

Figure 5. The NOE build-up curves constructed from three NOESYs at 500 MHz as described in the text. The graph shows the relative NOE intensity of selected intramolecular DNA cross peaks: (●) C1C5H→C1C6H, (■) C3C5H→C3C6H, (◆) C9C5H→C9C6H, (▲) C11C5H→C11C6H, and intermolecular DNA to BIGBEN cross peaks: (○) A5C2H→CH_3-1 and A17C2H→CH_3-2, (□) A6C2H→CH_3-1 and A18C2H→CH_3-2, (◇)T20C1′H→CH_3-1 and T8C1′H→CH_3-2. (A) The relative intensity of all selected intra- and intermolecular cross peaks and (B) an expansion showing the weak relative intensity of the selected intermolecular cross peaks.

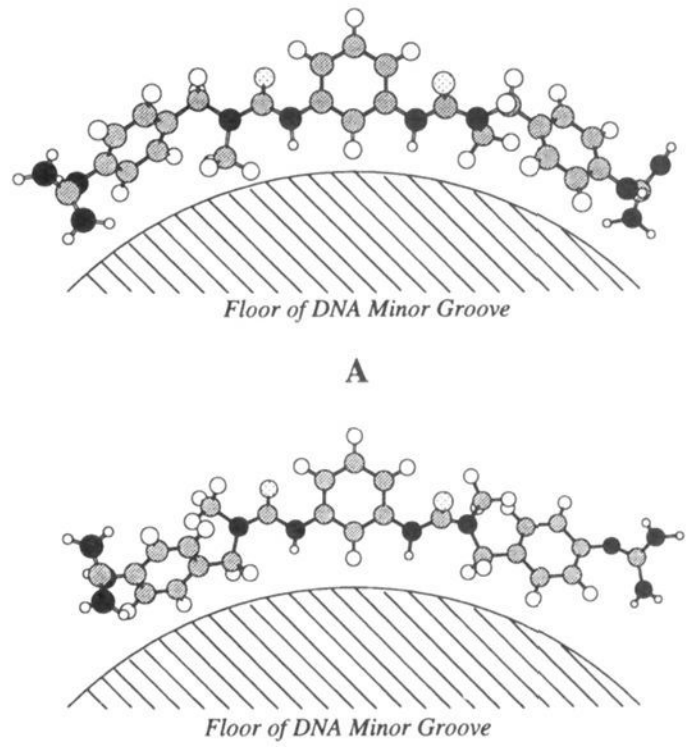

Figure 6. (A) The "Methyl in" conformation of BIGBEN and (B) The "Methyl out" conformation of BIGBEN. The black atoms are nitrogen, the dark striped atoms are carbon, the light stippled atoms are oxygen, and the white atoms are hydrogens.

When this N-Me out conformation of BIGBEN is docked into the minor groove of the dodecamer, the methylene groups of the ligand are proximal to the floor of the minor groove, potentially involved in favorable van der Waals interactions with the DNA. Indeed, the *N*-methyl groups were added to BIGBEN in the design process to allow for such an *N*-Me out conformation; omission of the methyl groups would produce a disubstituted urea moiety in which the benzyl group would be fixed *cis* to the carbonyl oxygen. In addition, the *N*-Me out conformation is analogous to the observed binding mode for distamycin and netropsin in that the methyl groups would be oriented away from the minor groove. In contrast, our NMR results clearly indicate a bound conformation of BIGBEN that places the urea *N*-methyl groups *trans* to the carbonyl oxygen. The ligand in the *N*-Me "in" conformation is represented schematically in Figure 6A.

Computational Models. We examined DOCK's ability to distinguish the observed *N*-methyl in conformation from the *N*-methyl out conformation. A representative starting structure was generated for both the *N*-methyl in and the *N*-methyl out conformations. These structures were DOCKed into the dodecamer, and the resulting configurations were subjected to AMBER minimization within the fixed field of the DNA receptor. The resulting minimized structures were then re-DOCKed into the DNA. Both conformations received very favorable final DOCK scores, but the observed *N*-methyl in conformation received a slightly more favorable score (−65 kcal/mol) than the *N*-methyl out conformation (−62 kcal/mol). The configuration of the *N*-methyl in conformation produced by DOCK corresponds to a translation of 4.1 Å and a rotation of 19° relative to the symmetric model. This corresponds to a shift in the binding site one base-pair along the minor groove. Indeed, the asymmetrical binding mode predicted by DOCK for the *N*-Me in conformation may reflect one of the two symmetry-related binding configurations of BIGBEN that are in fast exchange on the NMR time scale as described below. A more thorough search of the conformational space available to BIGBEN led us to examine 16 000 low energy conformations but did not produce any conformations that received more favorable scores than either the *N*-Me in or the *N*-Me out conformations.

The observation of fast chemical exchange precludes a quantitative interpretation of the NOE data. The data interpretation requires the aid of a model, beginning with the simplest and working up to a level of complexity required for consistency with the experimental data. The averaged NOEs were thus used with computational modeling to determine which structural models are likely, in accordance with established procedures.[40] We describe two models of the interaction between BIGBEN and d(CGCGAATTCGCG)$_2$ that were built to determine which more accurately represents the observed data.

(a) Symmetric Model. The simplest model was built to address the retention of symmetry and the observed NOEs. This model was also useful to investigate the ability of the originally selected binding site 5′AATT3′ to satisfy the observed NOEs. The ligand is located centrally in the minor groove with the symmetry axis passing through the H2-2 and H5-2 protons. Molecular modeling revealed that the NOEs satisfied by this model are as follows: H2-2→A6C2H, A18C2H, T8C1′H, and T20C1′H; CH_3-1→A5C2H, A6C2H, T7C1′H, and T20C1′H, CH_3-2→A17C2H, A18C2H, T19C1′H, and T8C1′H. This places the NH-2 and NH-3 protons within hydrogen bonding distance of the A5N3, T20O2 and T8O2, A17N3 atoms, respectively. The proximity of two hydrogen bond acceptors to one hydrogen bond donor implies that the formation of bifurcated hydrogen bonds is possible similar to those observed in netropsin and distamycin.[41−43] None of the ligand's other donor hydrogens are within acceptable hydrogen bonding distance from the DNA's acceptor atoms. An examination of further possible interactions with the centrally bound ligand implies that electrostatic interactions are likely between the terminal guanidiniums and opposing phosphates. However, with the ligand centrally bound we cannot explain the simultaneous NOEs between the NH-1→C21C4′H and NH-4→C9C4′H

(41) Newton, M. D.; Jeffrey, G. A.; Takagi, S. *J. Am. Chem. Soc.* **1979**, *101*, 1997−2002.
(42) Kopka, M. L.; Yoon, C.; Goodsell, D.; Pjura, P.; Dickerson, R. E. *J. Mol. Biol.* **1985**, *183*, 553−563.
(43) Klevitt, R. E.; Wemmer, D. E.; Reid, B. R. *Biochemistry* **1986**, *25*, 3296−3303.

protons. With the ligand centrally bound the distance between the NH-1 and the C21C4′H protons is about 7.0 Å, as is the distance between the NH-4 and C9C4′H protons. In addition, the H2-2→A6C4′H and A18C4′H NOE cannot be satisfied as this distance is *ca.* 10 Å in the centrally-bound model.

(b) **Offset Model.** A more satisfactory model is generated if we presume that as the ligand exchanges off and on the binding site it binds in two symmetry-related off-center binding sites. We note in this regard that we cannot distinguish between an "on-and-off" or a "back-and-forth" mechanism of exchange. We used this assumption that two symmetry related binding sites exist along with the information gained from the reDOCKing of the ligand to the DNA to determine an offset model of interaction. One of the sites corresponds to a shift in the ligand towards the 3′ end of the plus strand, such that the binding site relative to this strand is 5′ATTC3′. The symmetry-related second binding site corresponds to a shift in the ligand toward the 3′ end of the minus strand. In each of these sites the ligand maintains its curvature and twist allowing it to mirror the curvature of the minor groove, a characteristic of many minor groove binders.[3] A schematic drawing of the ligand in its two symmetry-related sites on the DNA and the NOEs which are satisfied is shown in Figure 7. As shown in Figure 7A the NH-4→C9C4′H NOE may be satisfied, while the ligand is in this site, in addition to the following NOEs being satisfied: CH_3-1→A5C2H, C21C1′H, and C21C4′H; H2-2→A6C2H, A6C4′H, and T20C1′H; NH-3→A6C2H and T20C4′H; CH_3-2→A6C2H, A18C2H, T7C1′H, T19C1′H, and T20C1′H; H2,6-3→A18C2H and C9C4′H; and the H3,5-2→A17C2H, A18C2H, and C9C4′H. The second site is illustrated in Figure 7B where the NH-1→C21C4′H NOE may be satisfied, while the ligand is in this site, in addition to the following NOEs being satisfied; CH_3-2→A17C2H, C9C1′H, and C9C4′H; H2-2→A18C2H, A18C4′H, and T8C1′H; NH-2→A18C2H, and T8C4′H; CH_3-1→A18C2H, A6C2H, T19C1′H, T7C1′H, and T8C1′H, H2,6-1→A6C2H and C21C4′H, and the H3,5-1→A5C2H, A6C2H, and C21C4′H. These models were examined carefully using Biosym software (data not shown) and account for every observed NOE. Further graphical analysis of the offset models reveals the possibility of three bifurcated hydrogen bonds between the ligand and the DNA instead of the two expected in the centrally-bound model. In Figure 7B, the NH-1 proton of the ligand is proximal to the A6N3 and T20O2 hydrogen bond acceptors, the NH-2 proximal to the T8O2 and A18N3 hydrogen bond acceptors, and the NH-3 proximal to the C9O2 and A17N3 hydrogen bond acceptors. In Figure 7A, the NH-4 proton of the ligand is proximal to the T8O2 and A18N3 hydrogen bond acceptors, the NH-3 proximal to the A6N3 and T20O2 hydrogen bond acceptors, and the NH-2 proximal to the A5N3 and C21O2 hydrogen bond acceptors.

The formation of the offset complex versus the symmetric complex is further supported by the results obtained from the deconvolution of the energies of interaction between the ligand and the DNA for the two complexes. The symmetric complex shows an interaction energy of −201.624 kcal/mol that consists of a nonbonded interaction energy of −49.679 kcal/mol, an electrostatic interaction energy of −150.520 and a hydrogen bond interaction energy of −1.325 kcal/mol. The offset complex shows an interaction energy of −225.472 kcal/mol that consists of a nonbonded interaction energy of −54.438 kcal/mol, an electrostatic interaction energy of −169.339, and a hydrogen bond interaction energy of −1.696 kcal/mol. Although our calculations are performed *in vacuo* and reflect static energies, they indicate that the offset model is energetically favored by about 25 kcal/mol versus the symmetric complex.

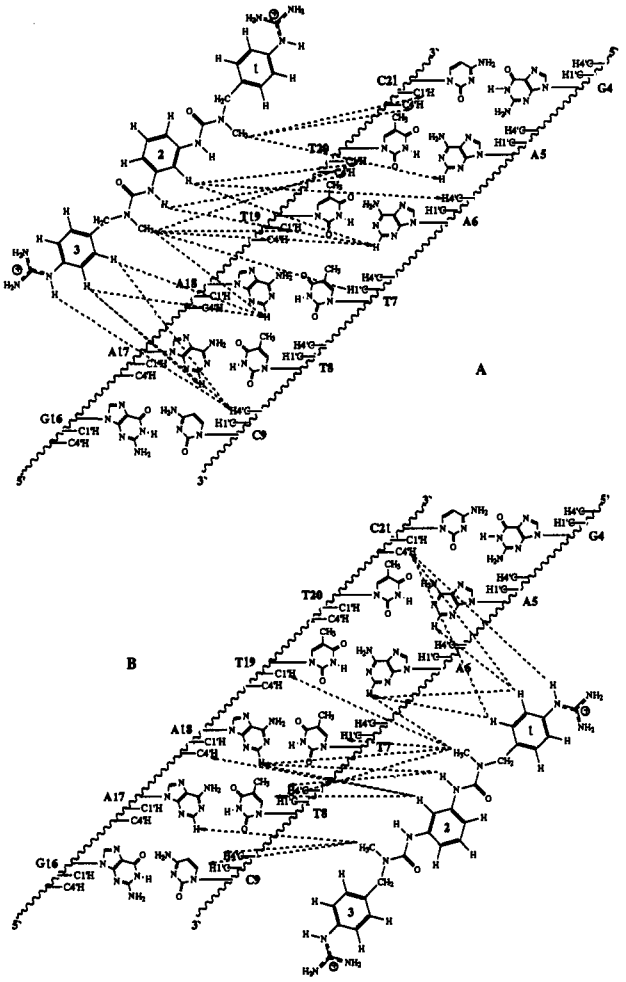

Figure 7. Schematic showing the summary of the intermolecular NOEs in a two-site, fast-exchange model. (A) The ligand is shifted towards the 3′ end of the minus strand. (B) The ligand is shifted towards the 3′ end of the plus stand. The NOEs satified in both (A) and (B) are described in the text.

Discussion

We have used NMR techniques to investigate the complex formed between a *de novo* designed DNA minor groove ligand, BIGBEN, and the receptor for which it was designed, the 5′AATT3′ site of the Dickerson dodecamer. Twenty intermolecular NOEs (40 if each symmetric pair of protons is considered distinct) between BIGBEN and the DNA clearly place the binding site in the AT rich region of the minor groove. Thermal denaturation studies have already established that BIGBEN exhibits a slight preference for binding to AT-rich regions in polymeric DNA.[7] Since monitoring the interaction between BIGBEN and DNA was hampered by the ligand's lack of a convenient chromophore the gross sequence selectivity was quantified using ethidium displacement techniques. By quantifying the amount of ethidium displaced from DNA upon addition of BIGBEN the apparent association constant of BIGBEN for both poly(dAdT)$_2$ and poly(dCdG)$_2$ was determined. Based on the apparent association constants, BIGBEN displays a slight preference for binding to poly(dAdT)$_2$. Although BIGBEN binds to poly(dAdT)$_2$ much more weakly than distamycin, its apparent association constant for this polymer compares favorably with the binding of other DOCK generated lead compounds to their corresponding receptors ($K = 10^5-10^3$ M^{-1}),[44]

(44) Kuntz, I. D.; Meng, E. C.; Shoichet, B. K. *Acc. Chem. Res.* **1994**, *27*, 117−123.

The titration data clearly indicate that the ligand·DNA complex is in fast chemical exchange with respect to chemical shift on the NMR time scale. This fast exchange behavior is not unique to BIGBEN and has been observed for several minor groove binding ligands with association constants for poly-(dAdT)$_2$ stronger and weaker than that of BIGBEN, two examples of which follow. Fast chemical exchange is observed throughout the titration for the symmetric ligand P1-F$_4$S-P1 which has an AT-rich DNA association constant of about 1×10^3 M^{-1},[45] This behavior is also displayed by the symmetric ligand berenil which has an AT-rich DNA association constant of about 1×10^6 M^{-1}.[29] In each of the two cases, fast exchange precludes the type of analysis that is possible for slow exchange ligands such as distamycin or netropsin. The combination of degenerate and nondegenerate resonances observed during the titration and subsequent NOE characterization of our complex is similar to the previously characterized behavior of P1-F$_4$S-P1, Hoescht 33258, and berenil. Although we observe fast exchange, the change from degenerate resonances free in solution to nondegenerate resonances in the presence of the receptor is an indication of the formation of a stable complex, as noted for the ligand P1-F$_4$S-P1, which binds about 100-fold less tightly than BIGBEN.[45] This is what occurs with the methylene protons (CH_2-1 and CH_2-2) of BIGBEN which are degenerate free in solution and become resolved, nondegenerate resonances in the presence of the oligonucleotide. In contrast, the proton resonance degeneracies of ring one (H2-1/H6-1 and H3-1/H5-1) and ring three (H2-3/H6-3 and H3-3/H5-3) of BIGBEN are an indication of rapid molecular motion around the carbon−carbon bond between the ligand's methylene and phenyl moieties similar to that observed for the phenol moiety of Hoescht 33258 when complexed to d(CGCGAATTCGCG)$_2$,[46] Although the phenol group of Hoescht 33258 is buried at the floor of the minor groove and its motions should be inhibited by the proximity of the DNA, rapid rotation appears to have little effect on the ligand DNA interaction and may be attributed to the ability of the DNA to dynamically "breath".[39] This behavior is also displayed by berenil which retains the degeneracy of the protons on its two phenyl rings,[29]

Examination of the chemical shifts of the BIGBEN−DNA complex indicates less perturbation then with some minor groove binding agents. It is common to observe larger chemical shift perturbations of not only minor groove but also major groove protons upon complex formation between a minor groove binding agent and its respective target sequence. This is especially true for ligands such as distamycin, Hoescht 33258, berenil, and netropsin which induce chemical shift changes upon formation of a ligand−DNA complex ranging from ± 0.1 to ± 1.10 both in the minor and major grooves.[29,43,46,47] The largest chemical shift change we observe is −0.22 ppm. The change in chemical shift can be attributed to at least several causes, a change in the geometry of both the ligand and receptor and a change in the proximity of moieties with large ring current effects,[43,48,49] Examination of the data for several complexes reveals that some of the largest changes in chemical shift occur not only in regions of the greatest structural perturbation and ligand-induced ring current effects but also in protons that are proximal to highly electronegative moieties. This behavior is exemplified by P1-F$_4$S-P1 complexed to d(CGCAAATTTGCG)$_2$ which has a AT-rich DNA association constant about 100-fold weaker than BIGBEN. Although only one DNA chemical shift perturbation was reported, it was for the A6C2H proton (+0.28 ppm) which is proximal to the ligand's central fluorine atoms.[45] Berenil shows greater chemical shift perturbations for several minor groove protons than the still tighter binding distamycin, although the berenil−DNA NOEs are very weak.[29] There thus appears to be little correlation between a ligand's association constant and the resulting perturbations in chemical shift of the complex, Berenil has a central NH-N=N moiety in closest proximity with the minor groove protons, which may be partly responsible for the greater chemical shift perturbation than we observe. Lane et al, also reported that berenil's rings are likely in closer contact with the floor of the minor groove than what we observe. In the case of another minor groove binder in fast exchange, SN 6999, heterocylic rings are in closer contact with the minor groove than the benzyl rings.[50] The constituent moieties of BIGBEN are not as electronegative (Figure 1), and the chemical shift data and observed pattern of NOEs indicates that its structural perturbation of the DNA is minimal. These electronegativity factors must contribute, as does the fact that for a complex in fast chemical exchange the chemical shift will be moderated by the rate of exchange and the observed value will be a mol fraction average of the free and bound resonance frequencies.

The NOE build up curve also reflects the fast chemical exchange and rapid molecular motions of the ligand. The exchange rate shortens the effective rotational correlation time of the nuclei undergoing the motion, which leads to a spread in the values of the effective τ_c for both the ligand and the receptor, This results in weak intermolecular NOEs even in the case of protons which are less than 5 Å apart. Our NOE build up curve is consistent with the NOE build-up simulations for reduced overall correlation times, In such simulations, protons that are known to be less than 5 Å apart in a DNA oligomer display weak NOE build-ups due to correlation times that are reduced, for example, *ca.* tenfold,[51] Weak intermolecular NOEs were also observed by Lane et al., between berenil and DNA, also in fast exchange and interpreted to be in close contact with the minor groove.[29] The observation of the BIGBEN's exchangeable protons only in the presence of the DNA and only between the ligand and the minor groove protons provides further support for our interpretation of close intermolecular proximity but averaged, weak NOEs,

The NOE results and the computational guided modeling of the complex show that BIGBEN does not bind to the oligonucleotide in the originally desired manner.[7] BIGBEN was designed to mimic the shape of the lead compound, 1,3,5-tris-(4-biphenylyl)benzene (Figure 1A), This design hypothesis was based on the fact that trisubstituted ureas are known to adopt a conformation in which the N−H and the carbonyl oxygen are oriented *trans*.[52] Rotation about the (O=C)-NR′R″ bond is facile, with an activation energy of less than 9 kcal/mol,[53] Molecular mechanics calculations of a 1-benzyl-1,3-dimethyl urea model system indicate that the difference between conformations having the 1-benzyl group *cis* versus *trans* with respect to the carbonyl oxygen is negligible (<0,2 kcal/mol). Thus, we expect that free in solution, the BIGBEN ligand exists as a rapidly interchanging mixture of *cis*−*trans* geometries corresponding to the *N*-methyl out and *N*-methyl in conformers,

(45) Wang, A. H.-J.; Cottens, S.; Dervan, P. B.; Yesinowski, J. P.; van der Marel, G. A.; van Boom, J. H. *J. Biomol. Struct. Dynam.* **1989**, *7*, 101−117.
(46) Parkinson, J. A.; Barber, J.; Douglas, K. T.; Rosamond, J.; Sharples, D. *Biochemistry* **1990**, *29*, 10181−10190.
(47) Patel, D. J. *Proc. Natl. Acad. Sci. U.S.A.* **1982**, *79*, 6424−6428.
(48) Pelton, J. G.; Wemmer, D. E. *Biochemistry* **1988**, *27*, 8088−8096.
(49) Giessner-Prettre, C.; Pullman, B. *Biopolymers* **1976**, *15*, 2277−2286.
(50) Leupin, W; Chazin, W. J; S. Hyberts; Denny, W. A.; Wuthrich, K. *Biochemistry* **1986**, *25*, 5902−5910.
(51) Wijmenga, S. S.; Mooren, M. M. W.; Hilbers, C. W. In *NMR of Macromolecules*; Roberts, G. C. K., Ed.; IRL Press: New York, 1993; pp 217−288.
(52) Stilbs, P. *ACTA Chemica. Scanda.* **1971**, *25*, 2635−2642.
(53) Stilbs, P.; Moseley, M. E. *J. Magn. Reson.* **1978**, *31*, 55−61.

respectively. As we have shown BIGBEN binds with the methyl groups pointed into the minor groove. In both the symmetric and offset models of the BIGBEN·dodecamer complex there are numerous favorable van der Waals interactions between the *N*-methyl groups and atoms on the floor of the minor groove. This situation is in fact not so different to that observed for distamycin and netropsin, where similar favorable van der Waals contacts are made between the pyrrole C−H groups, the terminal amidine methylene group and the floor of the minor groove.[48] Similar favorable van der Waals interactions are the sole source of the noncovalent sequence recognition by the minor groove ligand CC-1065 with the dodecamer studied here.[54] It is likely that there are additional effects that stabilize the bound *N*-methyl in conformer of BIGBEN. We hope to delineate such contributions by studying the binding of BIGBEN to a nonsymmetric oligomer.

Due to the fast chemical exchange behavior we are unable to determine a high resolution structure and can only offer models of the interaction between BIGBEN and the oligonucleotide. As we have shown, we use information in addition to the NOE to show that the offset binding model is the most accurate representation of the bound behavior of BIGBEN. The evidence for this comes from a variety of observations and computational results. The first of these is the chemical shift perturbation data. The data indicate that the greatest change in chemical shifts are located at the minor groove protons of residues A6/A18 through C9/C21 suggesting a 5′ATTC3′ rather than a 5′AATT3′ binding site. This indicates that the ligand does not effectively "see" the DNA as a symmetric binding site but favors the 3′ terminus of either strand. Corroborating support for this model comes from the results obtained from the reDOCKing of the ligand to the DNA in the *N*-methyl in conformation. This indicates that the preferred binding site should be shifted one base pair in either the 5′ or 3′ direction from the originally proposed 5′AATT3′ binding site. Finally we have carefully examined the structural characteristics of the two models. It is evident that the offset model can more accurately account for all of the observed NOEs as well as having more favorable electrostatic and hydrogen bonding interactions. The symmetric model, while instructive for examing the possible interactions, cannot account for all of the NOEs and has some moieties poorly positioned for interactions with the minor groove. The deconvoluted energies of interaction also display this preference for the offset model although they must be interpreted with a high degree of caution since they do not represent a true ensemble average of the interaction.

We thus propose a model of interaction where the DNA has two symmetry related 5′ATTC3′ (=5′GAAT3′ on the opposing strand) binding sites with the ligand in fast chemical exchange. Such a model is consistent with the data we present herein and the interpretation of other fast-exchange ligand-DNA complexes in the literature.[29,45,50] We cannot yet distinguish between a model in which the ligand slides back-and-forth or flips end-to-end, as has previously been noted for such complexes in fast exchange. The fast exchange rate decreases the effective τ_c and results in a relatively weak signal and longer build up time for the intermolecular NOEs. Our interpretation also has the ability to explain the observed slight line broadening since the asymmetric binding footprint would cause an asymmetry in the ligand·DNA complex and a slight change in the chemical shift of a previously degenerate resonance to a nondegenerate resonance. In the fast chemical exchange regime this effect could not be directly observed, and the resulting resonances would be observed as being a slightly broadened average signal.

(54) Scahill, T. M.; Hansen, M.; Hurley, L. H. 1994, personal communication.

Conclusion

We have used homonuclear 2D NMR to show that BIGBEN binds exclusively to the AT rich region of the minor groove of d(CGCGAATTCGCG)$_2$. This represents the first complete cycle of our structure based design cycle applied to the minor groove of DNA. The difference observed between the conformation of BIGBEN assumed in the design process and that observed in the complex between BIGBEN and the dodecamer demonstrates a limitation of the DOCK program as we have employed it; no allowance is made for the conformational flexibility of the ligand or the receptor DNA. Based upon these observations, we are investigating the DNA binding of bis-*N*-des-methyl-BIGBEN. This analog lacks BIGBEN's *N*-methyl groups which are involved in favorable van der Waals interactions with the floor of the minor groove in the BIGBEN·d(CGCGAATTCGCG)$_2$ complex observed here. Preliminary foot printing data indicate that the bis-*N*-des-methyl-BIGBEN binds tighter to AT-rich regions than BIGBEN (unpublished data). Although several iterations of the design cycle may be necessary to compete with the tight binding of natural products, our contribution shows the feasibility of this approach. In addition, our results clearly illustrate the centrally important role that NMR plays in this cyclic design strategy.

Acknowledgment. Financial support was provided in part by the U.S. Public Heath Service, Grant GM50892 (to S.M.K.) and GM39552 (to I.D.K. and G.L.K.). D.A.K. thanks the Graduate College at the University of Minnesota for financial support, Dr. Vikram Roongta and the Biomedical Engineering/Biochemistry NMR Center at the University of Minnesota for continued support, Drs. Vladimir Basus, Daina Avizonas, and Shauna Farr-Jones for assistance with the 600 MHz NMR at UCSF, and Dr. Jeffrey Pelton and Professor David Wemmer for helpful discussions. C.R.W. was supported in part by the NIH Molecular Biophysics Training Grant 5T32 GM08277-07.

Supporting Information Available: Amber force field parameters of BIGBEN (atom types and charges, bond parameters angle parameters, and dihedral parameters) (1 page). This material is contained in many libraries on microfiche, immediately follows this article in the microfilm version of the journal, can be ordered from the ACS, and can be downloaded from the Internet; see any current masthead page for ordering information and Internet access instructions.

JA943618F